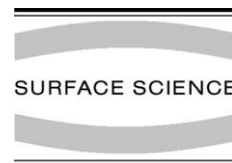




ELSEVIER

Available online at [www.sciencedirect.com](http://www.sciencedirect.com)

Surface Science xxx (2003) xxx–xxx

[www.elsevier.com/locate/susc](http://www.elsevier.com/locate/susc)

# Fabrication and characterization of novel semiconductor nanomechanical structures

Hiroshi Yamaguchi<sup>a,\*</sup>, Yoshiro Hirayama<sup>a,b</sup>

<sup>a</sup> NTT Basic Research Laboratories, NTT Corporation, 3-1 Morinosato-Wakamiya, Atsugi-shi, Kanagawa 243-0198, Japan

<sup>b</sup> CREST, JST, Kawaguchi, Saitama 331-0012, Japan

## Abstract

As an application of the “*bottom-up*” self-organization growth technique to the fabrication of nanoscale mechanical structures, we selectively etched a GaAs sacrificial layer under InAs wires preferentially grown on bunched steps on misoriented GaAs(1 1 0) surfaces, which led to the successful formation of single crystal InAs nanoscale cantilevers. The lengths, widths, and thicknesses of the *nanolevers* are typically 50–300, 20–100 and 10–20 nm, respectively. The force constant, as measured by the force-modulation imaging technique using contact-mode atomic force microscopy, ranges from 0.5 to 10 N/m, showing good agreement with that estimated from the elastic constant of InAs. The resonance frequency is expected to reach 500 MHz for the smallest one, which promises possible application to high-speed nanomechanical devices.

© 2003 Published by Elsevier Science B.V.

**Keywords:** Atomic force microscopy; Molecular beam epitaxy; Gallium arsenide; Indium arsenide; Semiconductor–semiconductor heterostructures

## 1. Introduction

Micro- and nanoelectromechanical systems (MEMS/NEMS) have the potential to bring about a revolution in the application of semiconductor fine-structure devices, such as high-resolution actuators and sensors, high-frequency signal processing components, and medical diagnostic devices [1,2]. Resonators [3–5], force detectors [6], accelerometers [7], magnetometers [8,9], and other highly sensitive sensors have been demonstrated using MEMS/NEMS devices. Also MEMS/NEMS

are important in the study of fundamental quantum physics. When the resonance frequency of a NEMS resonator becomes sufficiently high as the result of size reduction, novel quantum mechanical functions are expected to emerge [1,10–12]. The typical scale of the resonator is  $100 \text{ nm} \times 10 \text{ nm} \times 10 \text{ nm}$ , where the energy quantum of the oscillator becomes a few electron volts, possibly being detectable in a dilution refrigerator [1]. Studies of macroscopic quantum tunneling [1,10,11] and the realization of mechanical entangled states [12] have been proposed based on the quantization of the mechanical degree of freedom.

State-of-the-art electron-beam lithography has been generally employed for the fabrication processes of NEMS structures [1–5]. Fabricating structures of this size while keeping crystalline

\* Corresponding author. Tel.: +81-46-240-3475/3311; fax: +81-46-240-4727.

E-mail address: [hiroshi@will.brl.ntt.co.jp](mailto:hiroshi@will.brl.ntt.co.jp) (H. Yamaguchi).

quality high is not straightforward because electron-beam lithography can damage the structure. As a possible alternative to this conventional technique, we propose a “*bottom-up*” approach for fabricating semiconductor nanomechanical structures, which is expected to provide both high crystalline quality and small device sizes [13]. This method uses the preferential growth of molecular-beam epitaxy of InAs on the bunched monomolecular steps on a GaAs substrate, which was originally proposed to fabricate semiconductor quantum wires for optoelectric applications [14]. In this paper, we demonstrate this novel fabrication technique and characterize the elastic properties of the fabricated nanomechanical cantilevers by force-modulation imaging using contact-mode atomic force microscopy (AFM).

## 2. Experimental results

Fig. 1 schematically illustrates the fabrication processes of the InAs nanoscale cantilevers (here-

after called *nanolevers*). The substrates were GaAs(110) wafers misoriented toward the (111)A direction by  $5^\circ$ . A 100-nm-thick GaAs buffer layer and a five-period GaAs/Al<sub>0.5</sub>Ga<sub>0.5</sub>As (30-nm-thick each) superlattice form the regular multi-step structures on the growth surface (Fig. 1(a)). InAs 5-nm thick was then deposited, resulting in the formation of InAs wires along the bunched steps (Fig. 1(b)). Then 5- to 10- $\mu\text{m}$ -wide mesas were defined by photolithographic patterning. Selective etching of sacrificial GaAs and AlGaAs layers was then performed using  $\text{NH}_4\text{OH}:\text{H}_2\text{O}_2:\text{H}_2\text{O} = 1:30:300$  solution and HF, respectively, to fabricate the InAs nanolevers (Fig. 1(c) and (d)).

Fig. 2 shows a SEM image of the fabricated InAs nanolevers. They are typically 50–300 nm long and 20–100 nm wide. The length uniformity was largely improved by the use of RIE dry etching compared with the previous results obtained with chemical wet etching [13]. The spacing between adjacent wires is 400–800 nm for this  $5^\circ$  misoriented samples and can be controlled by adjusting the misorientation angle. With further se-

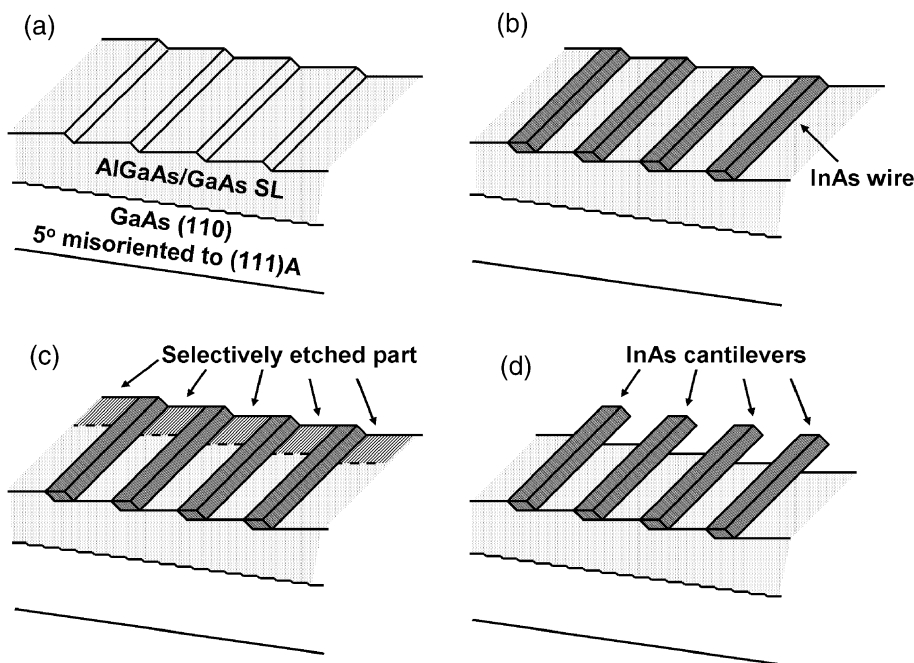


Fig. 1. Schematic illustration of the fabrication process of InAs nanoscale cantilevers. (a) After the growth of GaAs/AlGaAs SL. A regular multi-step structure is formed. (b) After the deposition of InAs. InAs wires are preferentially grown at the multi-steps. (c) After the lithographic patterning of mesa stripes. (d) After the selective etching of GaAs/AlGaAs SL to form the InAs nanoscale cantilevers.

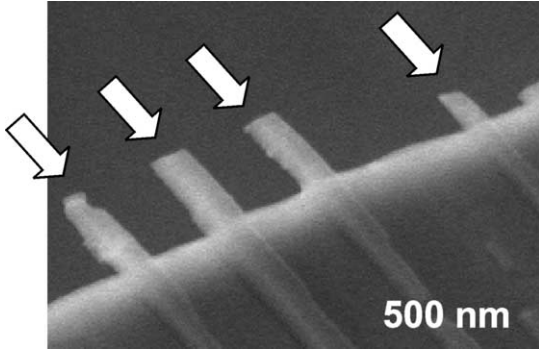


Fig. 2. SEM image of the samples after the selective etching of the GaAs sacrificial layer.

lective etching, the nanolevers stick to the surface. It is expected that this can be prevented by applying a critical point dryer [15].

The thickness of the nanolever was measured by means of SEM observation and ranged from 10–20 nm depending on the amount of deposited InAs. One of the main advantages of using InAs for the electromechanical structures is the accumulation of native electrons in the near-surface region due to surface Fermi level pinning in the conduction band [16,17]. In other single-crystal semiconductors, where the surface Fermi level is pinned in the band gap, carriers are depleted when the membrane thickness is reduced to the nanometer scale. In contrast, electrons accumulate in InAs nanolevers if the lowest quantum level formed in the nanolever is lower than the pinning position of surface Fermi level. This condition is given by  $E_F > \hbar^2(t^{-2} + w^{-2})/8m_e$ , where  $t$  and  $w$  are the thickness and the width of the InAs nanolever, respectively,  $m_e$  is the effective mass of conduction electron,  $\hbar$  the Planck's constant, and  $E_F$  the position of surface Fermi level. The vacuum barrier is assumed to be infinitely high for simplicity. The second term in the parenthesis can be neglected because  $w \gg t$  in our structures. Using the reported value of 0.15 eV for  $E_F$  [16,18] and  $0.026m$  for  $m_e$ , we estimated the critical thickness for electron accumulation is 9.8 nm. This estimation is roughly consistent with those obtained in the scanning tunneling spectroscopy [18] and angle-resolved photoelectron spectroscopy studies [19], both of which reported that the critical

thickness of electron accumulation is 5–6 nm for InAs/GaAs(111)A heterostructures. Because the electron is more easily accumulated in the free-standing InAs membranes than the heterostructures [17], we expect that the fabricated InAs nanolevers are all electrically conductive even when they are thinner than 10 nm.

The elastic properties of the InAs nanolevers were then characterized by force-modulation imaging by contact-mode AFM [20,21]. We detected the change in the deflection of the AFM cantilever scanned over the sample surface while applying sample-height modulation with the  $z$ -piezo-translator. The local force constant on the sample surface,  $c_s$ , is given by

$$c_s = c \delta z_c / (\delta z_s - \delta z_c), \quad (1)$$

where  $c$  is the force constant of the AFM cantilever,  $\delta z_s$  the sample height modulation, and  $\delta z_c$  the induced deflection of the AFM cantilever. For an ideal rectangular cantilever beam, the force constant  $c_s$  is given by

$$c_s = Ewt^3/4l^3, \quad (2)$$

where  $E$  is Young's modulus and  $l$ ,  $w$  and  $t$  are the length, width and thickness of the cantilever, respectively. For our measurements, we chose  $c$  of 0.08 N/m, chosen to be more than 10 times smaller than  $c_s$ . Therefore, combining Eqs. (1) and (2), one can approximately obtain

$$\delta z_c \sim \delta z_s (1 - 4cl^3/Ewt^3). \quad (3)$$

Therefore, the measured InAs nanolever deflection,  $\delta z_c - \delta z_s$ , is proportional to the third power of distance from the cramped position.

Fig. 3 shows a typical topographic image (a) and stiffness map (b) of two InAs nanolever. The signal voltage from the photodetector, which is sensing and proportional to the AFM cantilever deflection  $\delta z_c$ , was mapped in Fig. 3(b). The sample height modulation  $\delta z_s$  is 0.2 nm. The complicated images beside the two nanolevers are due to the finite curvature of the AFM cantilever tip. The dark contrast corresponding to reduced stiffness induced by the elastic deflection of InAs nanolever is clearly visible. The contrast becomes darker at larger distances from the nanolever support.

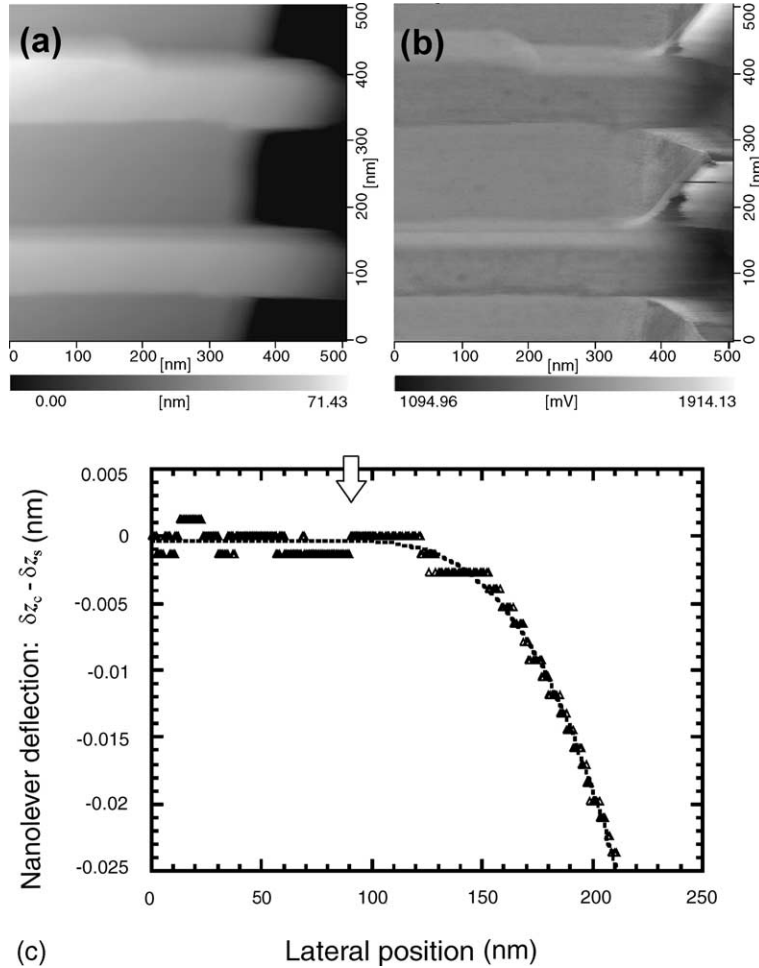


Fig. 3. (a) A topographic image and (b) a stiffness map for two fabricated InAs nanolevers obtained by contact-mode AFM characterization. (c) Nanolever deflection plot along the nanolever length axis. The arrow shows the clamped position of the nanolever. The dotted line is the fitting curve obtained by assuming Eq. (3).

Fig. 3(c) plots the measured InAs nanolever deflection,  $\delta z_c - \delta z_s$ , as a function of the lateral position, i.e. along the length axis of the nanolever. As shown in Eq. (3), the deflection is proportional to the third power of the distance from the cramped position. The fitting of this curve determines the nanolever force constant as obtained by Eqs. (2) and (3).

The evaluated force constants of 14 nanolevers are plotted as a function of measured nanolever width in Fig. 4. For the comparison among these

different nanolevers, the force constant was normalized using the standard nanolever length of 100 nm, i.e. we plotted the evaluated value of Eq. (2) at  $l = 100$  nm. It ranges from 0.5 to 10 N/m depending on the size of nanolever. The dashed lines show the force constants calculated from Eq. (2) with Young's modulus of bulk InAs,  $E_{\text{InAs}} = 5.2 \times 10^{10}$  N/m<sup>2</sup>, for four different values of nanolever thickness. The thickness range shows good agreement with the previous SEM observation, justifying our force constant measurement

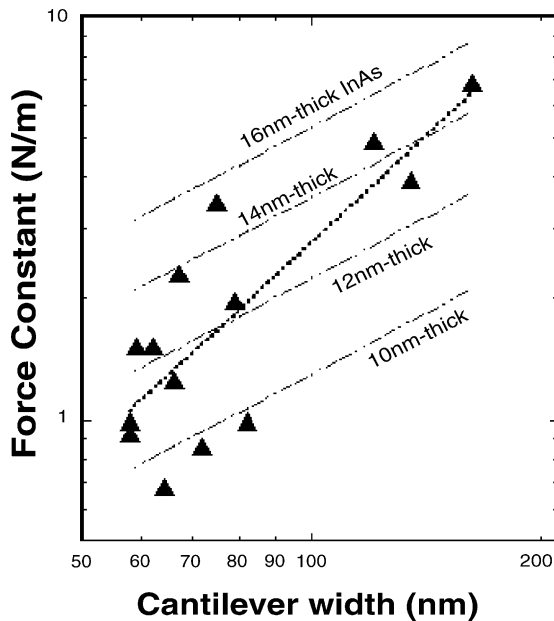


Fig. 4. Force constants 100 nm from the clamped position evaluated from the fitting of nanolever deflection–position plot (Fig. 3(c)) for 14 different cantilevers. The dashed line shows force constants calculated from the nanolever dimensions and elastic constant of bulk InAs.

technique. The data shows that the thickness tends to slowly increase with nanolever width as indicated by the dotted line. The line corresponds to the relation of  $t \sim w^{0.25}$  which might indicate some scaling nature of InAs wire growth on the bunched steps. Finally, the resonant frequency  $f$  of a cantilever can be estimated from

$$f = (1.875)^2 t (E/12\rho)^{1/2} / 2\pi l^2, \quad (4)$$

where  $\rho$  is the density of the material ( $5.7 \times 10^3 \text{ kg/m}^3$  for InAs). For the fabricated InAs nanolever, the estimation gives the resonant frequency ranging from 30 to 500 MHz, which promises possible application to high-speed nanomechanical devices.

### 3. Conclusion

We have successfully fabricated an InAs nanoscale cantilever array by using a “bottom-up” self-organization growth technique. The force constant of fabricated cantilevers was determined by a

force-modulation imaging technique using contact-mode AFM. The obtained force constant shows good agreement with the estimation from the bulk InAs elastic constant.

### Acknowledgements

The authors are grateful to Dr. Sunao Ishihara and Dr. Takaaki Mukai for their encouragement throughout this work. This work was partly supported by the NEDO International Joint Research Program “nano-elasticity”.

### References

- [1] M.L. Roukes, in: Technical Digest of the 2000 Solid-State Sensor and Actuator Workshop, 2000, p. 1.
- [2] H.G. Craighead, *Science* 290 (2000) 1532.
- [3] A.N. Cleland, M.L. Roukes, *Appl. Phys. Lett.* 69 (1998) 2653.
- [4] D.W. Carr, S. Evoy, L. Sekaric, H.G. Craighead, J.M. Parpia, *Appl. Phys. Lett.* 75 (1999) 920.
- [5] A. Erbe, H. Krommer, A. Kraus, R.H. Blick, G. Corso, K. Richter, *Appl. Phys. Lett.* 77 (2000) 3102.
- [6] T.D. Stowe, K. Yasumura, T.W. Kenny, D. Botkin, K. Wago, D. Rugar, *Appl. Phys. Lett.* 71 (1997) 288.
- [7] E.B. Cooper, E.R. Post, S. Griffith, J. Levitan, S.R. Manalis, M.A. Schmidt, C.F. Quate, *Appl. Phys. Lett.* 76 (2000) 3316.
- [8] B.C. Stipe, H.J. Mamin, T.D. Stowe, T.W. Kenny, D. Rugar, *Phys. Rev. Lett.* 86 (2001) 2874.
- [9] J.G.E. Harris, D.D. Awschalom, F. Matsukura, H. Ohno, K.D. Maranowski, A.C. Gossard, *Appl. Phys. Lett.* 75 (1999) 1140.
- [10] A.N. Cleland, M.L. Roukes, in: 24th International Conference on the Physics of Semiconductors, World Scientific, Singapore, 1999.
- [11] S.M. Carr, W.E. Lawrence, M.N. Wybourne, *Phys. Rev. B* 64 (2001) 220101.
- [12] A.D. Armour, M.P. Blencowe, K.C. Schwab, *Phys. Rev. Lett.* 88 (2002) 148301.
- [13] H. Yamaguchi, Y. Hirayama, *Appl. Phys. Lett.* 80 (2002) 4428.
- [14] S. Torii, K. Bando, B.-R. Shim, K. Maehashi, H. Nakashima, *Jpn. J. Appl. Phys.* 38 (1999) 4673.
- [15] H. Namatsu, K. Yamazaki, K. Kurihara, *Microelectron. Eng.* 46 (1999) 129.
- [16] V. Heine, *Phys. Rev. A* 138 (1965) 1689; J. Tersoff, *Phys. Rev. Lett.* 52 (1984) 465.
- [17] H. Yamaguchi, R. Dreyfus, Y. Hirayama, S. Miyashita, *Appl. Phys. Lett.* 78 (2001) 2372.

- [18] H. Yamaguchi, Y. Hirayama, *Jpn. J. Appl. Phys.* 37 (1998) 1599;  
H. Yamaguchi, J.L. Sudijono, B.A. Joyce, T.S. Jones, C. Gatzke, R.A. Stradling, *Phys. Rev. B* 58 (1998) R4219.
- [19] H. Åskland, L. Ilver, J. Kanski, S. Mankefors, U. Södervall, J. Sadowski, *Phys. Rev. B* 63 (2001) 195314.
- [20] P. Maivald, H.J. Butt, S.A.C. Gould, C.B. Prater, B. Drake, J.A. Gurley, V.B. Elings, P.K. Hansma, *Nanotechnology* 2 (1991) 103.
- [21] R. Biesendanger, *Scanning Probe Microscopy and Spectroscopy*, Cambridge University Press, Cambridge, 1994, p. 240.